Mechanics and Mechanical Engineering
Vol. 17, No. 1 (2013) 99–112

Static and Dynamic Thermomechanical Buckling Loads of Functionally Graded Plates

Katarzyna Kowal–Michalska
Radosław J. Mania
Department of Strength of Materials
Łódź University of Technology
Stefanowskiego 1/15, 90–924 Łódź, Poland

Received (11 March 2013)
Revised (16 April 2013)
Accepted (20 May 2013)

In the paper the buckling phenomenon for static and dynamic loading (pulse of finite duration) of FGM plates subjected to simultaneous action of one directional compression and thermal field is presented. Thin, rectangular plates simply supported along all edges are considered. The investigations are conducted for different values of volume fraction exponent and uniform temperature rise in conjunction with mechanical dynamic pulse loading of finite duration.

Keywords: Functionally graded plates, thermomechanical loadings, stability, pulse load.

1. Introduction

Functionally Graded Materials (FGM) were first introduced in 1984 by a group of Japanese scientists and very soon have become very popular in research and engineering applications. A typical FG gradient material is inhomogeneous composite made up of two constituents – typically of metallic and ceramic phases which relative content changes gradually across the thickness of a plate or a shell. This eliminates the adverse effects between the layers (e.g., shear stress concentrations and/or thermal stress concentrations), typical for layered composites. The high resistance heat capacity of ceramic and good mechanical properties of metal phase make that the leading application area of FGM structures are high temperature environments (spacecraft, nuclear reactors or structures for the chemical industry and defence) [13], [14].

Nonlinear analysis of plates and shells devoted to basic types of loads is covered in Shen monograph [14]. He considered static bending and thermal bending as an introduction to buckling and postbuckling behaviour of FGM plates and shells. The shear deformation effect is employed in the framework of Reddy's higher order shear deformation theory (HSDT).

In [13], alongside HSDT for FGM plates Reddy presents the comparison of FSDT and CLP theories application for functionally graded plates. According to presented results it is obvious that for thin–walled plates as well as for greater exponent value in the power law through the thickness distribution function [7], the application of FSDT gives results in practice the same as HSDT. The discrepancy between both theories is of 2% in calculated deflections of analyzed plates.

The static buckling problem of functionally graded plates is discussed in the frame of different approaches e.g.: in [16], [17] – biaxial in–plane compression and thermal loads (constant temperature) with axial compression, in [2] and [10] – biaxial in–plane compression, in work [3] – for thermal stresses only and in [12] – for through the thickness temperature gradient.

In mentioned above publications the dominant subject are the static mechanical or steady–state thermal loadings. The dynamic types of analyses concern mostly the vibrations problems. From our previous experience [6], [8] connected with static and dynamic analysis of thin–walled isotropic and orthotropic composite plates, the dynamic buckling of thin–walled structure is theoretically difficult problem but of great importance for practical engineering applications.

The present work deals with static and dynamic stability of thin rectangular plates, simply supported along all edges, made of functionally graded materials. The material properties are assumed to be temperature independent. Considered plates are subjected to static or dynamic uniaxial compression and uniform temperature rise, constant through the thickness and constant in time. The uniform temperature rise is of constant increment form.

The investigations are conducted by analytical methods for static case and numerical ones for dynamic pulse compression.

2. Description of FGM properties

According to the rule of mixture the properties of functionally graded material (ρ - density, α - coefficient of thermal expansion, E - Young's modulus, ν - Poisson's ratio) can be expressed as follows [1]:

$$\begin{aligned} &\rho(z) = \rho_m + (\rho_c - \rho_m)\left(\frac{2z+h}{2h}\right)^q; \quad \alpha(z) = \alpha_m + (\alpha_c - \alpha_m)\left(\frac{2z+h}{2h}\right)^q \\ &E(z) = E_m + (E_c - E_m)\left(\frac{2z+h}{2h}\right)^q; \quad \nu(z) = \nu_m + (\nu_c - \nu_m)\left(\frac{2z+h}{2h}\right)^q \end{aligned} \tag{1}$$

where $-h/2 \leq z \leq h/2$, and $q \geq 0$ is the volume fraction exponent (i.e., if $q = 0$ – plate is full ceramic and for $q = \infty$ – plate is metallic).

In this paper it is assumed that for a given fraction exponent q Poisson's ratioν is constant and equal to:

$$\nu = \frac{\int_{-h/2}^{h/2} \nu(z)dz}{h} \tag{2}$$

3. Subject of consideration

A square simply supported FG plate (Fig. 1) subjected simultaneously to uniform compression in x direction and uniform temperature rise is considered. The unloaded edges of plate are immovable. The coordinate system x, y, z coincides with the midplane of a plate.

It was proved in the paper [3] that for thin plates (a/h >40) the differences in the results obtained on the basis of classical laminate plate theory (CLPT) and FDST are less than 1÷2%. Therefore in this paper CLPT is employed to obtain the governing equations of thin FG plate equilibrium.

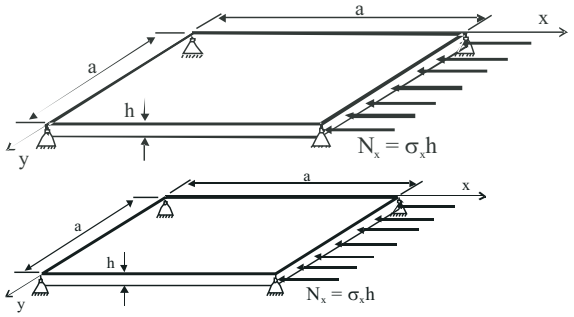

Figure 1 Geometry and loading of a plate

In the classical nonlinear laminate plate theory the strains across thickness are expressed referring to the displacements u, v and w of plate middle surface [4], [5]:

$$\{\varepsilon\} = \left\{\varepsilon^{(m)}\right\} + z\left\{\varepsilon^{(b)}\right\} \tag{3}$$

$$\{\varepsilon^{m}\} = \left\{\frac{\partial u}{\partial x} + \frac{1}{2}\left(\frac{\partial w}{\partial x}\right)^{2'} \quad \frac{\partial v}{\partial y} + \frac{1}{2}\left(\frac{\partial w}{\partial y}\right)^{2}, \quad \frac{\partial u}{\partial y} + \frac{\partial v}{\partial x} + \frac{\partial w}{\partial x}\frac{\partial w}{\partial y}\right\}^{T} \tag{4}$$

$$\left\{\varepsilon^{(b)}\right\} = \left\{-\frac{\partial^2 w}{\partial x^2}, \quad -\frac{\partial^2 w}{\partial y^2}, \quad -2\frac{\partial^2 w}{\partial x \partial y}\right\}^{T} \tag{5}$$

Taking into account the generalized Hooke's law for plane stress state, the in-plane stress and moment resultants ($\mathbf{N}$, $\mathbf{M}$) are defined as:

$$\begin{Bmatrix} \mathbf{N} \\ \mathbf{M} \end{Bmatrix} = \begin{bmatrix} \mathbf{A} & \mathbf{B} \\ \mathbf{B} & \mathbf{D} \end{bmatrix} \begin{Bmatrix} \varepsilon^{(m)} \\ \varepsilon^{(b)} \end{Bmatrix} \tag{6}$$

where: **A, B, D,** – are extensional, coupling and bending stiffness matrices, respectively, for FG plate of components listed below:

$$
\begin{aligned}
A_{11} = A_{22} &= \int_{-h/2}^{h/2} \frac{E(z)}{1-\nu^2} dz \\
A_{12} = A_{21} &= \int_{-h/2}^{h/2} \frac{E(z)}{1-\nu^2} \nu_d z \\
A_{66} &= \int_{-h/2}^{h/2} \frac{E(z)}{2(1+\nu)} dz \\
B_{11} = B_{22} &= \int_{-h/2}^{h/2} \frac{zE(z)}{1-\nu^2} dz \\
B_{12} = B_{21} &= \int_{-h/2}^{h/2} \frac{zE(z)}{1-\nu^2} \nu dz \\
B_{66} &= \int_{-h/2}^{h/2} \frac{zE(z)}{2(1+\nu)} dz \\
D_{11} = D_{22} &= \int_{-h/2}^{h/2} \frac{z^2E(z)}{1-\nu^2} dz \\
D_{12} = D_{21} &= \int_{-h/2}^{h/2} \frac{z^2E(z)}{1-\nu^2} \nu dz \\
D_{66} &= \int_{-h/2}^{h/2} \frac{z^2E(z)}{2(1+\nu)} dz
\end{aligned}
\tag{7}
$$

Due to the presence of nontrivial matrix **B**, the coupling between extensional and bending deformations exists as it is in case of unsymmetrical laminated plates [4].

The stretching–bending coupling affects strongly the constitutive equations and boundary conditions that have complex form and the solution procedures become difficult.

In some papers (e.g., [20]) the concept of 'physical neutral surface' is introduced that allows to uncouple the in–plane and out–of–plane deformations.

The position of this physical neutral surface in the adopted coordinate system:

$$
e = -\frac{B_{11}}{A_{11}} \tag{8}
$$

can be found, assuming that under pure bending a surface exists for which strains and stresses are zero.

The displacements u, v, w corresponding to x, y, z axes take the following forms:

$$u = u_0 - \frac{\partial w}{\partial x}(z-e), \quad v = v_0 - \frac{\partial w}{\partial y}(z-e), \quad w = w(x,\, y) \tag{9}$$

where: u_0, v_0, w are displacements of physical neutral surface.

Strains are defined as:

$$\{\,\varepsilon\} = \left\{\,\varepsilon^{(0)}\right\} + (z-e)\left\{\,\varepsilon^{(1)}\right\} \tag{10}$$

The relations defining the in-plane stress and moment resultants in function of strains, have now the following form:

$$\left\{\begin{array}{c}\mathbf{N}\\ \mathbf{M}\end{array}\right\} = \left[\begin{array}{cc}\mathbf{A} & 0\\ 0 & \mathbf{D}^*\end{array}\right]\left\{\begin{array}{c}\varepsilon^{(0)}\\ \varepsilon^{(1)}\end{array}\right\} \tag{11}$$

The components of extensional stiffness matrix **A** are given by the relation (7) and for bending stiffness matrix **D*** are as follows:

$$D_{11}^* = D_{22}^* = D_{11} - \frac{B_{11}^2}{A_{11}}; \qquad D_{12}^* = D_{21}^* = \nu D_{11}^*; \qquad D_{66}^* = \frac{1-\nu}{2}D_{11}^* \tag{12}$$

Comparing relations (**??**) with laminate plate theory based on geometric middle plane, it can be seen that there is no extensional-bending coupling in constitutive equations of equilibrium of FG plate subjected to in-plane compression and these equations are the same as for homogenous isotropic plate.

4. Stability under static thermomechanical loadings

The well known Bubnov–Galerkin method has been applied to the problem solution. The procedure is classical and described in details in many works concerning stability of isotropic, composite and FGM plates (e.g. [5], [7], [8], [16]).

The plate is simply supported along all edges and the boundary conditions have been assumed as follows:

for loaded edges $x = 0, a$:

$$w = M_x = 0; \quad u_0 \neq 0 \qquad N_x = \sigma_x^h \qquad N_{xy}^{=} 0; \tag{13}$$

for unloaded edges $y = 0$, a:

$$w = M_y = 0; \quad v_0 = 0 \qquad N_y = 0 \qquad N_{xy} = 0. \tag{14}$$

The deflection function is taken in the form:

$$w = f \sin\frac{\pi x}{a}\sin\frac{\pi y}{a}. \tag{15}$$

and after rather long elaborations, the relation among compressive stress σ_x, increment of uniform temperature rise ΔT and nondimensional deflection amplitude $f* = f/h$ has been obtained:

$$\sigma_x = \sigma_{x0} + \frac{4B_{11}}{a^2(1+\nu)} f* + \frac{\pi^2 A_{11} h}{4a^2(1+\nu)} f*^2, \tag{16}$$

where:

$$\sigma_{x0} = \frac{4\pi^2 D*}{a^2 h(1+\nu)} - \frac{K\Delta T}{1+\nu} \tag{17}$$

and

$$K = \frac{1}{(2q+1)(q+1)} \left[\alpha_m(2E_m q^2 + E_c q) + \alpha_c(E_m q + E_c(q+1)\right] \tag{18}$$

The relation (16) has been compared with the relation derived in the paper [16] for a rectangular plate and the perfect agreement has been found.

Table 1 Constituents properties of considered metal–ceramic material [18]

	aluminium – TiC		aluminium–alumina	
ρ [kg/m^3]	2700	4920	2700	3950
E [GPa]	69	480	69	380
ν [-]	0.33	0.20	0.33	0.30
α [1/K]	$2.3{\cdot}10^{-5}$	$0.7{\cdot}10^{-5}$	$2.3{\cdot}10^{-5}$	$0.74{\cdot}10^{-5}$

4.1. *Calculations results*

Some calculations have been performed for FG square plates of ratio width to thickness equal to: $a/h = 60$ and 80 and temperature increment $\Delta T = 20$ K and 40 K (only for $a/h = 60$). The material properties of components are given in Tab. 1.

Table 2 Values of bifurcational stress σ_{xo} (Eq. 17)

		σ_{xo}	[MPa]
q	ΔT[K]	$a/h = 60$	$a/h = 80$
0	20	295.0	93.40
	40	253.0	-
0.5	20	158.61	62.04
	40	96.50	-
1.0	20	117.50	41.47
	40	61.22	-
10	20	54.20	17.55
	40	24.63	-
∞	20	23.15	2.73
	40	-	-

From the results presented in Tab. 2 (values of bifurcational stress σ_{xo}) and in Figs. 2 and 3 (postbuckling curves), the influence of fraction volume exponent and the assumed value of temperature increment is clearly visible. For greater values of q (e.g. $q = 10$) the plate ability to sustain the compressive load at given ΔT is several times smaller than for a plate containing more ceramics (e.g. $q = 0.5$). As it can be seen the growth of temperature increment results in the decrease of compressive load.

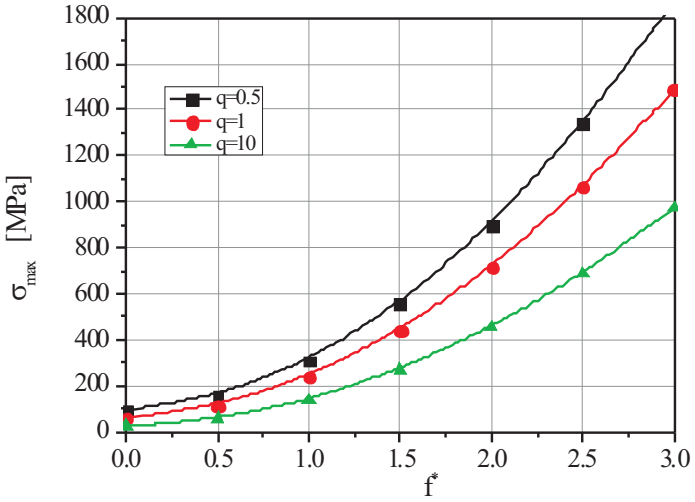

Figure 2 Postbuckling curves for FG plates of $a/h = 60$ and $\Delta T = 40$ K

It should be mentioned that equations (17) and (18) enable to find out the values of ΔT_{cr} and postbuckling curves as a function of uniform temperature rise versus non dimensional maximal deflection $f*$ at assumed value of compressive stress σ_x (see [16]).

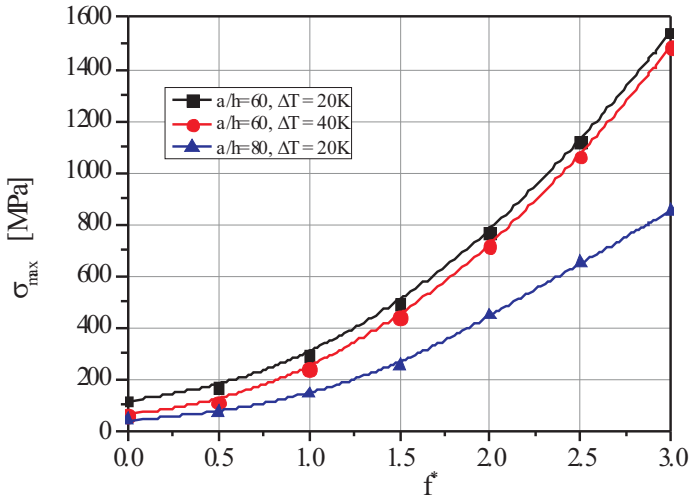

Figure 3 Postbuckling curves for FG plates ($q = 1$) of $a/h = 60$ ($\Delta T = 20$ K, 40 K) and $a/h = 80$ ($\Delta T = 20$ K)

5. Dynamic response of FG plate subjected to pulse compressive load and constant uniform temperture rise

For plates and plate structures, it is structures with stable postbuckling path, opposite to the static loading the bifurcational dynamic buckling load does not exist. The dynamic buckling is considered as a result of an in–plane load which involves rapid deflections growth of plate/walls, which is/are initially not flat but imperfect. It has been proved that for pulses of short duration the structure can withstand the dynamic loading magnitude much greater than the static one. The dynamic pulse buckling occurs for pulses of intermediate amplitude and duration close to the period of fundamental natural flexural vibration. Due to lack of bifurcation load it is necessary to define a "critical" load on the basis of an assumed dynamic buckling criterion. In most publications the Budiansky–Hutchinson criterion [6] is applied to determine the dynamic critical load that is the amplitude of pulse load, which at given duration causes the dynamic buckling. Dynamic buckling criterion of Budiansky–Hutchinson states that: *dynamic stability loss occurs, when the maximal plate deflection grows rapidly with the small variation of the load amplitude.*

Its modified version was employed for thermal buckling analysis as well [15], where author used it to determine the buckling temperature.

The dynamic load factor DLF is introduced, defined as the ratio of amplitude of pulse load to the critical static buckling load for ideal structures. Its critical value DLF_{cr} can be estimated on the basis of Budiansky–Hutchinson criterion.

In their previous work [7] the authors presented the dynamic buckling analysis of thin FG rectangular plates, subjected to in plane compressive pulse loading.

The boundary conditions in dynamic buckling analysis are assumed likewise in the previous static considerations i.e., all plate edges are simply supported. The plate is subjected to in–plane compressive pulse load of rectangular shape, of duration T_p equal to the period of fundamental flexural vibrations T_0 of considered FG plate and simultaneously there is under one of two thermal environmental conditions. The first one is define as $\Delta T = 20$ K and next $\Delta T = 40$ K, following those of static solution. The thermal condition $\Delta T = 0$ K solution compared with results of work [7] can be treated as validation procedure. Beside sets of thermal environmental conditions the dynamic pulse load was referred to two reference planes distinguish by condition ([7]).

6. FEM model of metal–ceramic plate

The numerical simulations and appropriate calculations have been conducted using the finite element software ANSYS [21]. The finite element SHELL181 has been used for discretisation of created multi–layered composite plate model. This is four nodes element with six degrees of freedom at each. It is suitable for analyzing geometrically nonlinear problems and modelling of different material properties. Its option *Shell SectionType* gives a possibility of defining a multi–layered cross–section, their thickness, number of integration points across each layer thickness and of introducing different material properties for separate layer. This approach of modelling FG plate as multi-layered one is common in FEM buckling analysis [7], [19]. However, there are known 3D approaches where the plate is modelled with application of solid finite elements with midside nodes [9].

The finite element SHELL181 is defined with respect to First Order Shear Deformation Theory what is in discrepancy with applied in analytical solution Classical Laminate Plate Theory. However for considered plate width to thickness ratio i.e. $a\ /\ h\ = 60$ and $a\ /\ h\ = 80$ the differences are negligible.

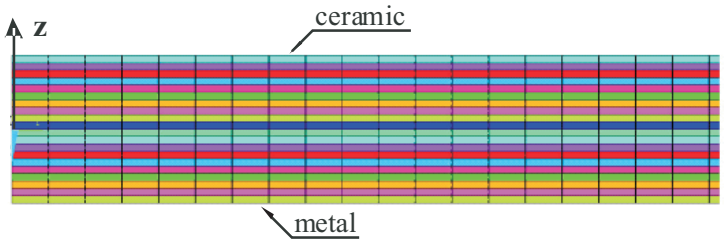

Figure 4 Plate multi–layered cross-section meshing

Preliminary considerations allowed establishing the mesh density, number of layers across the thickness of FG plate in order to obtain converged solution within acceptable time of computations. This analysis has shown that for a square plate the optimal discretisation corresponds to division into 50×50 elements of uniform mesh and 20 layers cross-section. The time step in applied Newmark time integration procedure has been taken as 1/50 of the period of plate fundamental natural vibration.

The boundary conditions following the analytical solution with assumption of simply support conditions, in finite element model were obtained through appropriate displacements constrains applied to nodes located at plate edges. Additionally, to achieve rectilinear shape of all edges translations normal to adequate edge of all its nodes were coupled. In the case of only thermal load all plate edges were kept unmovable.

7. Results of FEM computations

The square plate modelled as it was described in precedent subchapter was subjected only to mechanical load. It was dynamic in-plane pulse compression and then $\Delta \mathrm{T} = 0$. The pulse was of rectangular shape and lasted in time equal to the period of plate fundamental natural vibrations. Despite other aims, the impact of imperfection sense i.e. its sign plus or minus, was especially considered [10]. The exemplary results of these investigations for the volume fracture exponent $q = 1.0$ for FGM made of Al–TiC, are presented in Figs. 5 and 6.

In both graphs there are two plots distinguished with black and red colours. One curve (black) was obtained for the case when the imperfection had the positive sign. It corresponded with the first buckling mode when the plate buckles into ceramic direction. The second curve (red) was determined for the case when the imperfection had opposite sign to the first buckling mode and the initial half–wave was directed into metal layer. The differences between both curves are clearly visible in both analyzed cases.

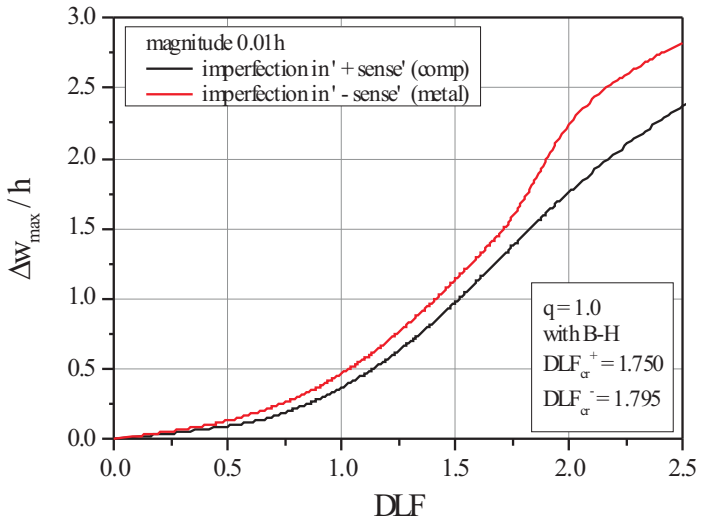

Figure 5 The influence of imperfection sense – low imperfection magnitude

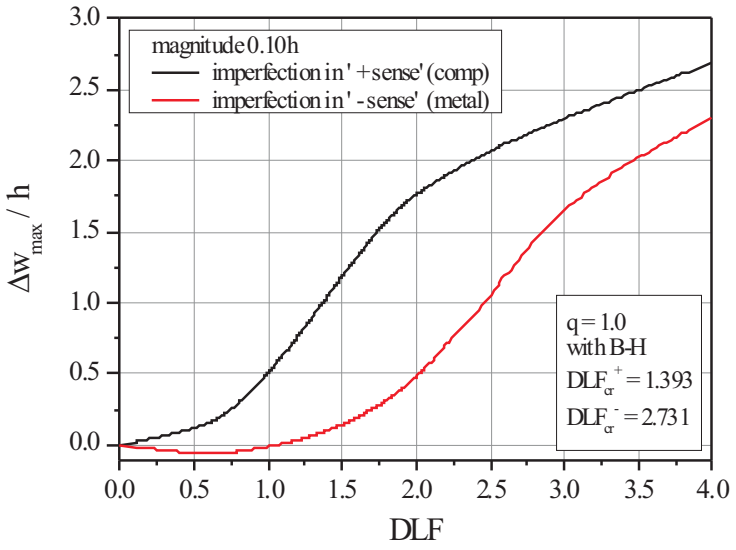

Figure 6 The influence of imperfection sense – high imperfection magnitude

The discrepancy between them increased for greater magnitude of imperfection. It leads as well to different values of dynamic critical load which values are given in legend frames included in both figures. For the greater imperfection magnitude equal to 0.1 of plate thickness, the critical *DLF* value for minus sign of imperfection is doubled of the second one. In reference to these results it should be reminded that homogenous isotropic plates are not sensitive to imperfection sign.

When the FGM plate is subjected to uniform temperature rise ΔT (with unmoveable edges) from the state of no thermal strains, the critical value of this increase can be determined when the plate buckles. As an example, for a square plate of unit thickness made of aluminium-alumina ($q = 1.0$) this value equals to $\Delta T_{cr} = 9.34$ K. However, the dependence of materials properties to temperature was neglected. Only their thermal expansion features were input into computational data.

During subsequent analysis the same plate was subjected to uniform temperature rise constant in time and simultaneously was dynamically loaded by compression pulse of finite duration. Similarly as in static analysis material properties of both constituents of functionally graded plate were defined as temperature independent. The applied thermal environmental conditions were closed to the critical temperature rise. The limits: $\Delta T = 8$ K and $\Delta T = 10$ K included the critical value ($\Delta T_{cr} = 9.34$ K). In Fig. 7 there are shown three plots obtained within this analysis.

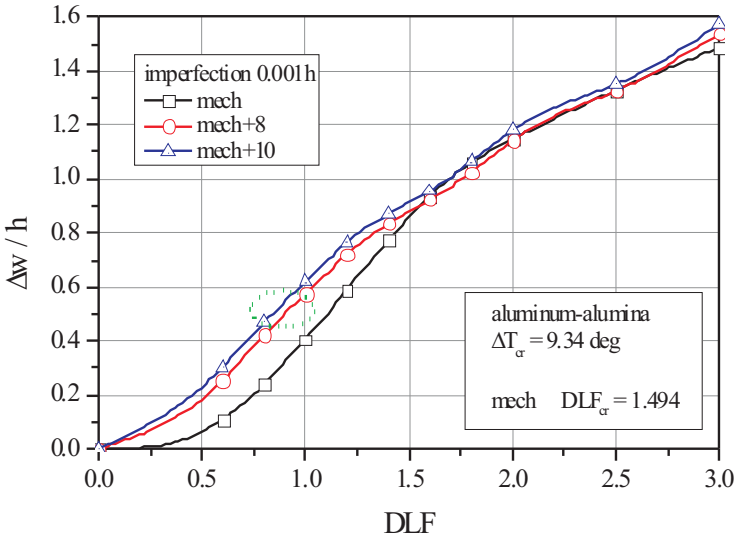

Figure 7 Dynamic response of FGM plate subjected to thermo–mechanical loads

The black line corresponds to only mechanical pulse load and presents the relationship between dynamic pulse amplitude *DLF* and normalized plate deflection. The next two were received for compound thermo–mechanical loads and also are function of plate deflection with respect to pulse magnitude. Determined with the

application of Budiansky–Hutchinson criterion the *DLF* critical value for pulse compression is less the 1.5. The critical values for combined thermo–mechanical loading can be estimated in the range marked in Fig. 7 with the circle. Both critical values are a bit lower than 1.0 what means significant decrease of dynamic critical load.

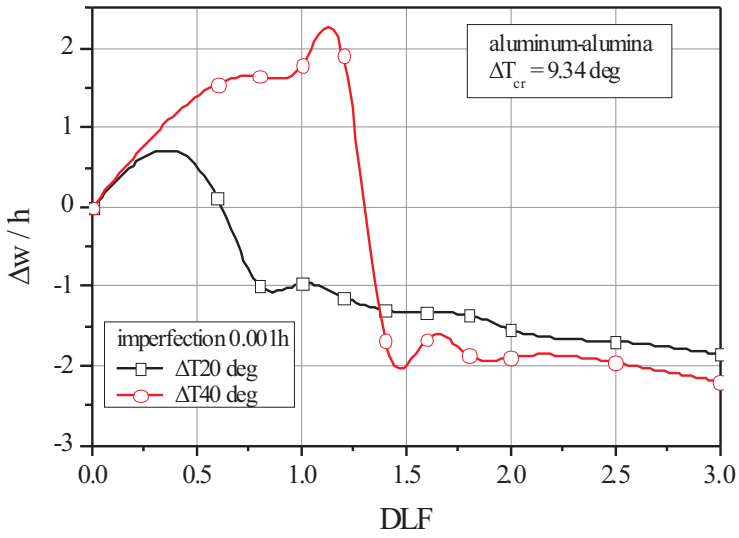

Figure 8 Dynamic response of FGM plate subjected to thermo–mechanical loads

For the cases when the thermal environmental conditions were apart from the critical condition ($\Delta T_{cr} = 9.34$ K) the computations were performed also for comparatively small initial imperfection amplitude (0.001 of plate thickness). These were two thermal uniform loads: $\Delta T = 20$ K and $\Delta T = 40$ K combined with compression mechanical dynamic pulse. Results of these calculations are presented in Fig. 8. The relationship of plots in this figure are the same as applied in previous graphs - $\Delta w/t = \mathrm{f}(DLF)$. The runs of these plots suggest that the plate dynamic response for these types of thermo-mechanical loads is dominated by bending not buckling. The deflection of plate caused by different thermal expansion of ceramic and metal layers added to mechanical type initial imperfection produces enough eccentricity for plate bending from the beginning of compression load.

8. Conclusions

The influence of thermal environmental condition with interaction of pulse loading on the dynamic response of FGM square plate was considered. The numerical results of this analysis were presented in appropriate figures.

The FGM plate is sensitive not only to imperfection magnitude but to its sense as well. This behaviour of plates made of FGM differs from homogenous isotropic plate response. Under combination of thermo–mechanical loading for relatively

small differences between applied thermal environment and critical conditions the bending participation predominate in dynamic response.

ACKNOWLEDGMENTS

This study is supported by the Ministry of Science and Higher Education in Poland – National Science Centre Grant No. ***2011/01/B/ST8/07441.***

References

[1] **Birman, V. and Byrd, L. W.**: Modeling and analysis of functionally materials and structures, *Applied Mechanics Review*, 60, 195–216, **2007**.

[2] **Bodaghi, M. and Saidi, A. R.**: Levy–type solution for buckling analysis of thick functionally graded rectangular plates based on the higher–order shear deformation plate theory, *Applied Mathematical Modeling*, 34, 3659–3673, **2010**.

[3] **Javaheri, R. and Eslami, M. R.**: Thermal buckling of functionally graded plates basing on higher order theory, *Journal of Thermal Stresses*, 25, 603–625, **2002**.

[4] **Jones, R. M.**: Mechanics of Composite Materials, 2nd ed., *Taylor & Francis*, London, **1999**.

[5] **Kołakowski, Z. and Kowal–Michalska, K. (eds)**: Selected problems of instabilities in composite structures, *A Series of Monographs*, Łódź, **1995**.

[6] **Kowal–Michalska, K. (ed.)**: Dynamic stability of composite plate structures, (*in Polish*), *WNT*, Warsaw, **2007**.

[7] **Kowal–Michalska, K. and Mania, R. J.**:Static and dynamic buckling of FGM plates, chapter 6, 131–151 in Królak, M. and Mania, R. J. (eds.), "Statics, dynamics and stability of structures", Vol. 1, "Stability of Thin–Walled Plate Structure", *A Series of Monographs*, Technical University of Łódź, **2011**.

[8] **Królak M. (ed.)**: Postbuckling states and ultimate load of thin–walled girders (*in Polish*), *PWN*, Warszawa–Łódź, **1990**.

[9] **Kyung–Su, N. and Ji–Hwan, K.**: Thermal postbuckling investigations of functionally graded plates using 3-D finite element method, *Finite Elements in Analysis and Design*, 42, pp. 749–756, **2006**.

[10] **Mania, R. J.**: Dynamic buckling of FGM thin–walled plate subjected to inplane bending, *Int. Conf. of Mechanics of Nano, Micro and Macro Composite Structure*, Torino, **2012**.

[11] **Naderi, A. and Saidi, A. R.**: On pre–buckling configuration of functionally graded Mindlin rectangular plates, *Mechanics Research Com.*, 37, 535–538, **2010**.

[12] **Prakash T., Singha M.K., Ganapathi M.**: Thermal postbuckling analysis of FGM skew plates, *Engineering Structures*, 30, 22–32, **2008**.

[13] **Reddy, J. N.**: Analysis of functionally graded plates, *Int. J. Num. Meth. Eng.*, 47, 663–684, **2000**.

[14] **Shen, H-S.**: Functionally Graded Materials – Nonlinear analysis of plates and shells, *CRC Press, Taylor & Francis*, London, **2009**.

[15] **Shariyat, M.**: Thermal buckling analysis of rectangular composite plates with temperature-dependent properties based on a layerwise theory, *Thin–Walled Structures*, 45, pp. 439–452, **2007**.

[16] **Tung, H-V. and Duc, N-D.**: Nonlinear analysis of stability for functionally graded plates under mechanical and thermal loads, *Composite Structures*, 92, 5, 1184–1191, **2010**.

[17] **Tsung–Lin, Wu, Shukla K. K. and Jin H. Huang**: Post–buckling analysis of functionally graded rectangular plates, *Composite Structures*, 81, 1–10, **2007**.

[18] **Tylikowski, A.**: Dynamic stability of functionally graded plate under in-plane compression, *Mathematical Problems in Engineering*, 2005–4, 411–424, **2005**.

[19] **Zhang, Y. X. and Yang, C. H.**: Recent developments in finite elements analysis for laminated composite plates, *Composite Structures*, 88, pp. 147–157, **2009**.

[20] **Zhou, D-G. and Zhou, Y-H.**: A theoretical analysis of FGM thin plate based on physical neutral surface, *Computational Material Science*, 44, 716–720, **2008**.

[21] **ANSYS ver. 12, Online manual**, SAS IP, Inc.